Experimental Investigation of Ash Deposit Behavior during Co-Combustion of Bituminous Coal with Wood Pellets and Empty Fruit Bunches

Tae-Yong Jeong [1], Lkhagvadorj Sh [1], Jong-Ho Kim [1], Byoung-Hwa Lee [2] and Chung-Hwan Jeon [1,3,*]

[1] School of Mechanical Engineering, Pusan National University, 2, Busandaehak-ro 63 beon-gil, Geumjeong-gu, Busan 46241, Korea; nautilus0@pusan.ac.kr (T.-Y.J.); lkhagva_1166@pusan.ac.kr (L.S.); rlawhdgh2001@pusan.ac.kr (J.-H.K.)
[2] Boiler R&D center, Doosan Heavy Industries and Construction, Volvoro 22, Seongsangu, Changwon 51711, Korea; byounghwa.lee@doosan.com
[3] Pusan Clean Coal Center, Pusan National University, 2, Busandaehak-ro 63 beon-gil, Geumjeong-gu, Busan 46241, Korea
* Correspondence: chjeon@pusan.ac.kr; Tel.: +82-51-510-3051; Fax: +82-51-510-5236

check for updates

Abstract: In Korea, oil-palm empty fruit bunches (EFBs), which are byproducts of the crude palm-oil milling process, are among the most promising potential energy sources for power plants. However, the slagging and fouling characteristics of EFBs during combustion have not yet been fully studied. Accordingly, in this study, we investigated the fundamental ash behavior of EFBs in comparison to that of wood pellets (WPs) using a thermomechanical analyzer (TMA) and a drop-tube furnace (DTF). Ash melting and the deposition of ash particles were investigated with traditional prediction indices at several biomass blending ratios. The results demonstrated that, as the ratio of WPs to EFBs increases, the melting temperature decreases and the slagging propensity increases because of the increased biomass alkali content. Moreover, the penetration derived using the TMA shows a higher melting peak at which rapid melting occurs, and the melting temperature distribution is decreased with increased biomass blending. Conversely, the DTF results show different phenomena for ash deposition under the same blending conditions. Blend ratios approaching 10% WP and 15% EFB result in gradual decreases in ash deposition tendencies because of the lower ash contents of the co-combusted mass compared to that of the single coal ash. Further biomass addition increases ash deposition, which is attributable to ash agglomeration from the biomass. Thus, this study demonstrates that blending ratios of 10% WP and 15% EFB provide optimal conditions for co-combustion with the selected bituminous coal. In addition, it is shown that the slagging propensity of EFB is higher than that of WP owing to its ash content and simultaneous agglomeration.

Keywords: biomass; co-combustion; ash deposition; ash melting behavior; agglomeration

1. Introduction

The burning of fossil fuels is a major cause of climate change owing to the massive greenhouse gas (GHG) emissions it entails. Many countries signed the Paris Agreement at the UN Climate Change Conference in 2015 with the aim of reducing GHG emissions. Consequently, these countries are developing alternative and renewable energy sources for fossil fuel replacement [1]. Biomass continues to grow in importance worldwide as a renewable and CO_2-neutral energy source that may help to diversify renewable energy sources for energy production [2].

The South Korean government has announced its intention to reduce greenhouse gas emissions by 37% before 2030 [3]. To achieve this target, the South Korean government has recommended the use of new and renewable energies for power generation, such as biomass, by the relevant companies at the national level through the renewable portfolio standard (RPS). Furthermore, the government plans to increase the supply of new and renewable energy fuels from 3% in 2015 to 10% by 2023 [4].

Biomass co-combustion or co-firing with coal is a potential strategy to achieve GHG abatement and reduce toxic emissions. Many previous studies have demonstrated that biomass co-firing can reduce net CO_2 emission because of the carbon neutrality of biomass, as well as decreasing NO_x and SO_x production [5,6]. This technology is favorable for many power plants because the fuel can be easily used in existing powdered coal-powered boilers without entailing any environmental or economic concerns [7,8].

Although biomass co-combustion and co-firing have the advantages of simple equipment configuration, low cost, and enhanced combustion performance, biomass fuels usually contain high levels of alkali and alkaline metals, particularly Na and K, which increase slagging and fouling in biomass-fired boilers [9].

For example, Baxter [10] studied ash deposition and slagging/fouling during the combustion of coal and biomass, and postulated a mechanistic model and ash deposition characteristics for biomass combustion. According to his results, the ash deposition phenomenon is associated with the combustion conditions and the type of inorganic material used for fuel co-combustion. He found that ash deposition by biomass peaks during initial combustion and then gradually decreases.

Pronobis [11,12] investigated the effects of co-firing a medium-level fouling coal with three types of biomasses on surface fouling in the convection region of a furnace. He revealed that the properties of the biomass fuel affect both the operation variables and the efficiency of the boiler. Furthermore, he co-fired two types of bituminous coals with different slagging tendencies and four types of biomasses (straw, wood, dried sewage sludge, and bone meal) and examined the slagging effect in the furnace in terms of the correlation between the properties and fusibility of the produced ashes. The results showed that co-firing increases the risk of slagging at the fireside in furnaces.

Theis et al. [13] co-fired peat and two biomass types (bark and straw) using an entrained-flow reactor and compared the resulting ash deposition with that of single-fired peat. They reported that the ash deposition rate does not increase, even when the bark and straw fuels are co-fired with peat at levels of 30 wt% and 70 wt%, respectively.

Savolainen [14] researched the slagging behavior of boilers by measuring and monitoring the soot-blowing frequency and attemperation of water flow. She reported that slagging and fouling in the furnace were maintained at normal levels despite co-firing with biomass.

Abreu et al. [15] co-combusted bituminous coals with two types of biomasses (pine sawdust and olive stones) at 10–50 wt% (according to calorific value) and examined the ash deposition rate. Co-combustion sawdust with a low alkali content led to a lower ash deposition rate than that observed for single-firing of coal. In contrast, co-combustion with olive stones with high K contents resulted in a higher ash deposition rate than that for single coal. They posited that this difference is caused by the different adhesion tendencies on the deposition surface and attributed this effect to the ash compositions of the biomasses.

In addition to the above studies, numerous studies have been performed to understand and explain the phenomenon of ash deposition in biomass co-combustion. This includes the development of empirical indicators and several experimental methods for determining ash melting temperatures [16–18]. Many investigations using thermomechanical analyzers (TMAs), drop tube furnaces (DTF), pilot plants, and full-scale boiler trials have been performed [19–21].

These previous studies have demonstrated that slagging and fouling propensities vary, particularly in response to type of blended fuel used. Recently, the use of oil-palm empty fruit bunches (EFBs) as biomass has been attempted in power plants in Korea for economic reasons. Thus, optimal operation parameters for the application of EFBs in power plants must be derived. Oil palms are widely cultivated

in tropical Asia, especially in Malaysia, Indonesia, and Thailand. Considering this abundant and CO_2-neutral fuel resource, oil-palm EFBs, as byproducts of the crude palm-oil milling process, represent one of the most promising energy resources [22,23].

There is much less literature available on the ash deposition behavior of EFBs compared to that on wood pellets (WPs) [24,25]. Thus, the goal of this study was to perform a detailed investigation into ash deposition during the co-combustion of pulverized coal with EFBs and WPs in pulverized form.

A bituminous coal from Australia with a relatively low slagging propensity was chosen as a representative fuel that is commonly used in Korean thermal power plants. The alterations in the extents and mechanisms of coal slagging were investigated during co-combustion with the two biomass types (WP and EFB). The ash melting characteristics and deposition rates were analyzed using a TMA and a DTF. In addition, X-ray fluorescence (XRF) analysis was performed to examine the chemical compositions of the ashes and derive their empirical prediction indices.

2. Materials and Methods

2.1. Sample Preparation

For this study, one type of bituminous coal typically used at domestic coal-fired thermal power plants and the two biomass types were used as fuels. Trafigura coal, a bituminous coal imported from Australia, served as the coal sample, and the WP and EFB were procured from Canada and Malaysia, respectively. In this paper, bituminous coal is indicated as T coal.

The coal and biomass samples were pulverized using a ball mill and sieved to particle sizes of 75–90 μm and 400–600 μm. These particle sizes are commonly employed in coal-fired power plants in Korea. Before the experiments, proximate and ultimate analyses of the samples were conducted using a TGA-701 system (LECO Co., St. Joseph, MI, USA) and TruSpec element analyzer (LECO Co., St. Joseph, MI, USA) in accordance with the relevant ASTM standards. The procedures specified in the standards ASTM D5142 and ASTM D3176 for coal and in standards ASTM E870 for the two biomasses, respectively. The calorific values were measured using an AC600 (LECO Co., St. Joseph, MI, USA) calorimeter. Table 1 shows the sample analysis results.

Table 1. Properties of selected samples.

Contents	Proximate Analysis (%wt. [a], Dry Basis)			Ultimate Analysis (%wt., Dry Ash Free Basis)					Heating Value (LHV [b])
	VM [c]	Ash	FC [d]	Carbon	Hydrogen	Nitrogen	Oxygen [e]	Sulfur	MJ/kg
Trafigura (AUS)	29.72	17.11	53.17	80.00	5.56	1.27	12.41	0.76	24.92
WP (CAN)	80.40	0.29	19.31	47.29	6.39	–	46.30	0.02	18.65
EFB (MAS)	76.49	2.77	20.74	47.67	5.75	0.12	46.43	0.03	18.50

[a] AUS: Australia, CAN: Canada, MAS: Malaysia, %wt.: % by weight, [b] LHV: low heating value, [c] VM: volatile matter, [d] FC: fixed carbon, [e] Oxygen: by difference.

In addition, ashes were fabricated in accordance with ASTM E1755-01 to examine their chemical compositions depending on the experimental conditions and their melting characteristics through TMA experiments. Accordingly, 1 g of sample dried at 105 °C was placed in a ceramic crucible and heated in a temperature-controlled muffle furnace. The sample was heated in an O_2 atmosphere from room temperature to 250 °C at 10 °C/min, and the temperature was maintained for 30 min. Then, the sample was heated again to 575 °C (±25 °C) at 20 °C/min and the final temperature was maintained for 3 h to obtain ash samples, from which the carbon contents of the fuels were completely removed at a lower ash-producing temperature than that of ASTM D1857. This procedure was employed to avoid the volatilization of inorganic materials by the flames during the early combustion process [17].

The chemical composition of each fabricated ash sample was analyzed with a PW2400 XRF (Philips Co., Eindhoven, The Netherlands) at the Korea Basic Science Institute based on the ASTM D4326 method.

2.2. TMA Experiments

TMA experiments are typically conducted to investigate the melting behavior of ashes from solid fuels [18,26]. This method is known to improve the reproducibility of experiments by removing the effects of operators that may be present in conventional ash fusion tests such as ASTM D1857. This method provides two important types of data that can be used to identify the slagging propensity of a fuel. The first data type is the penetration tendency of the ram into the sample, which is expressed as a function of temperature. The second data type is the penetration rate according to temperature, which is expressed as "peak". The peak denotes the maximum penetration rate for a given temperature change. This peak indicates the temperature range within which the rapid melting of the ash sample occurs, and it is derived from the first derivative of the penetration trace [27].

Figure 1 shows a schematic of the TMA used in this study. The TMA apparatus is composed of a heating chamber and penetrating rod, as well as a ram, crucible, linear variable differential transformer (LVDT), and thermocouple. The experimental procedure used in this study was as follows:
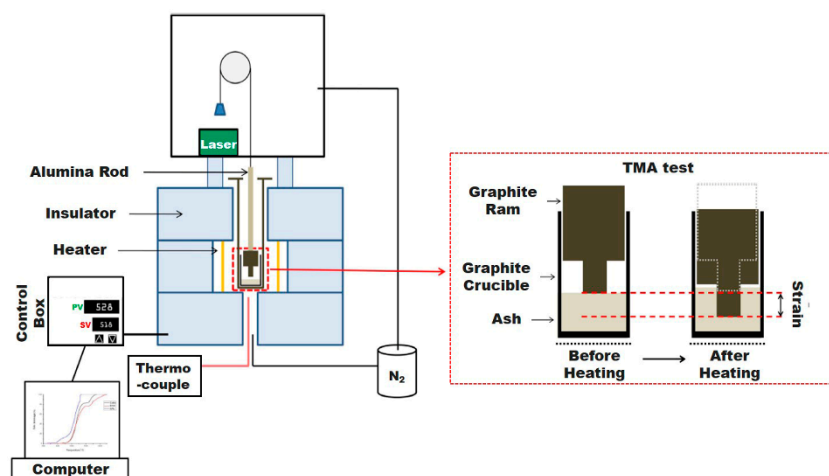

Figure 1. Schematic of the thermomechanical analyzer (TMA) apparatus.

Approximately 200 mg of an ash sample was placed in a crucible and the top of the sample was flattened with a jig by applying a constant pressure of 260 kPa. The sample was arranged in the prepared sample assembly by setting the pressure between the ram and the flattened sample surface at 30 kPa with a load of 60 g. The sample was then placed in a furnace. The sample was heated in a high-purity N_2 atmosphere. The furnace was first heated from room temperature to 600 °C at 50 °C/min, and then slowly heated at 5 °C/min from 600 °C to 1600 °C.

As shown in Figure 1, the ram sinks as the ash melts during the heating process, and the melted ash flows between the ram and the empty space in the bottom of the crucible when the ash is fully melted. The sinking displacement of the ram is measured with a laser displacement meter. This displacement indicates the height change of the ash sample from room temperature to a specific temperature and is converted to % shrinkage to evaluate the penetration of each sample according to temperature. The % shrinkage is used to identify the ash fusibility, which can be used as a predictor of ash deposition.

In addition, the peak at a specific temperature is determined from the first derivative of the % shrinkage. Generally, the peak distribution of a solid fuel shows more than two peaks, with each peak indicating rapid melting, i.e., melting acceleration intensity [28]. In this study, the peaks obtained from the shrinkage curves were differentiated at intervals of 10 min (or 50 °C) to prevent data scattering.

Gupta et al. [28] noted that temperatures of T25%, T50%, T75%, and T90% exhibit representative melting characteristics among the shrinkage values measured by the TMA in the melting of ash.

As the label suggests, T25% refers to the temperature at which the ash sample reaches 25% shrinkage. In this case, the 25% (±15%) liquid phase appears by the softening and sintering of ash. Specifically, it can be regarded as the cause of the initial ash deposition growth because the ash particles are sticky. At T50%, the ash has shrunk by 50% and approximately 60% (±15%) melting occurs. At T75%, over 80% melting occurs, and this temperature is judged to denote complete melting. It is known that boilers must operate at temperatures lower than T75% to allow the discharge of fly ash without it melting. Finally, T90% is regarded as the final stage of melting (liquid phase > 90%). This temperature represents the slag flow (or fluid flow) characteristics of the ash.

2.3. DTF Experiments

To examine the ash deposition tendencies according to the type of coal and biomass co-combustion, a DTF apparatus (600 mm long with an internal diameter of 70 mm) was used [29]. Figure 2 shows schematics of the DTF apparatus and deposition probe. The DTF apparatus used in this study was designed to simulate operation variables such as heating rate and gas temperature applied to the pulverized fuel boiler in actual coal-fired thermal power plants and to mount an ash deposition probe to indicate the ash deposition characteristics of the solid fuels. The deposited ash particles were captured in an alumina tube (60 mm long with an outer diameter of 25 mm) with a hollow cylindrical shape mounted at the end of the probe and inserted perpendicular to the gas flow inside the DTF apparatus. The ash deposition probe was positioned 10 cm upstream from the back of the DTF apparatus. The particles captured by the probe had relatively low carbon contents (<1% unburned carbon) and were protected from heat by the coolant supplied externally to the water jacket inside the probe. The temperature inside the DTF was maintained at approximately 1300 °C, and the total gas flow rate, comprising a mixture of O_2 and N_2, was 5 L/min. Furthermore, the feeding rate of the sample into the DTF during deposition experiments was 0.2 g/min over 1 h, and this rate was chosen to compensate for supply errors made by the screw feeder mounted on top of the DTF. These errors are caused by two phenomena. The first is supply retention by the screw feeder at the beginning of the experiment due to the densely packed samples, and the second is rate reduction at the end of the experiment due to the loosely packed samples, leading to decreased self-loading of fuel particles. The rate of air transport was adjusted so that the excess O_2 content was maintained at 1.16 (*v/v*, dry), the typical furnace exit value for pulverized fuel boilers [29]. The mass of deposited ash particles was obtained by calculating the difference between the clean and fouled samples, and this value was used to derive the deposit growth rates.
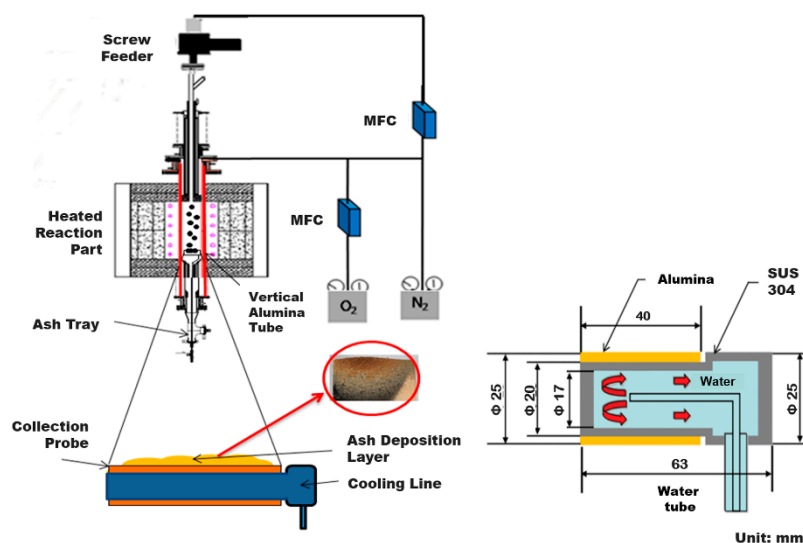

Figure 2. Schematic of the drop-tube furnace (DTF) apparatus and deposit probe (MFC: Mass flow controller; SUS: Steel use stainless).

In particular, to evaluate the ash deposition by biomass co-combustion at the same power output as that achieved with coal alone, the experiments were conducted based on the calorific value of T coal, which is similar to that of the coal typically used in actual domestic power generation boilers. The relevant conditions are illustrated in Figure 3, and the blend conditions for coal and biomass were customized using the thermal fraction of the biomass, as seen in Equations (1)–(3).

$$T_{fB} = \frac{\dot{m}_B Q_B}{\dot{m}_B Q_B + \dot{m}_C Q_C}; \ \left(T_f = T_{fB} + T_{fC}\right), \tag{1}$$

$$M_{fB} = \frac{\dot{m}_B}{\dot{m}_B + \dot{m}_C}; \ \left(M_f = M_{fB} + M_{fC}\right), \text{ and} \tag{2}$$

$$A_{fB} = \frac{\dot{m}_B A_B}{\dot{m}_B A_B + \dot{m}_C A_C}; \ \left(A_f = A_{fB} + A_{fC}\right). \tag{3}$$
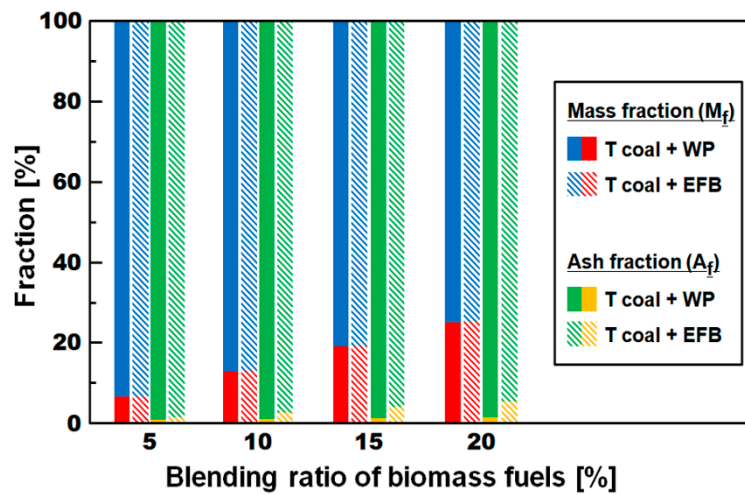

Figure 3. Blending conditions by thermal fractions of blends.

Here, T_f, M_f, and A_f denote the thermal, mass, and ash fractions by the proportions of the blends, respectively. Q, A, and $\dot{m}$ are the low heating value, ash content on dry basis, and mass flow (subscripts B and C denote biomass and coal), respectively.

Furthermore, the capture efficiency (CE) and energy-based growth rate (GRE) were derived to compare the ash deposition characteristics for the single and blended conditions from the deposition results obtained through five or more repeated experiments. The equations used for the calculations are as follows [30,31]:

$$CE = \frac{m_D}{m_A \times \left(\frac{A_C}{A_R}\right)} \times 100 \text{ and} \tag{4}$$

$$GRE = \frac{m_D}{LHV \times m_F}, \tag{5}$$

where m_D, m_A, and m_F denote the weight (g) of the deposit accumulated in the tube, total fly ash flowing towards the tube in the reactor, and blends fed during the test, respectively. A_C and A_R are the projected areas of the coupon and the cross-section of the DTF, respectively. These indices were derived from the weight of the collected particles acquired during the deposition experiment, and the measured weight was normalized to explain the difference in the fuel feeding rate.

3. Results and Discussion

3.1. Ashes from the Laboratory Experiments and Actual Combustion

The chemical composition of the ashes was analyzed to predict their deposition behaviors. In particular, to prevent the volatilization of the minerals generated from the initial biomass combustion process, separate analyses were conducted for the laboratory ash fabricated at a low temperature (575 °C) and the combustion ash obtained through the DTF experiment at a high temperature (1300 °C). For all the fuels fired, the char burnout in the combustion ash is always higher than 99% when the carbon content of the ash does not exceed 5%. The XRF results in Table 2 and Figure 4 show the chemical compositions of the laboratory/combustion ash and the propensity for slagging/fouling derived from several traditional indices. Table 3 presents the formulae and criteria pertaining to traditional prediction indices for ash deposition.
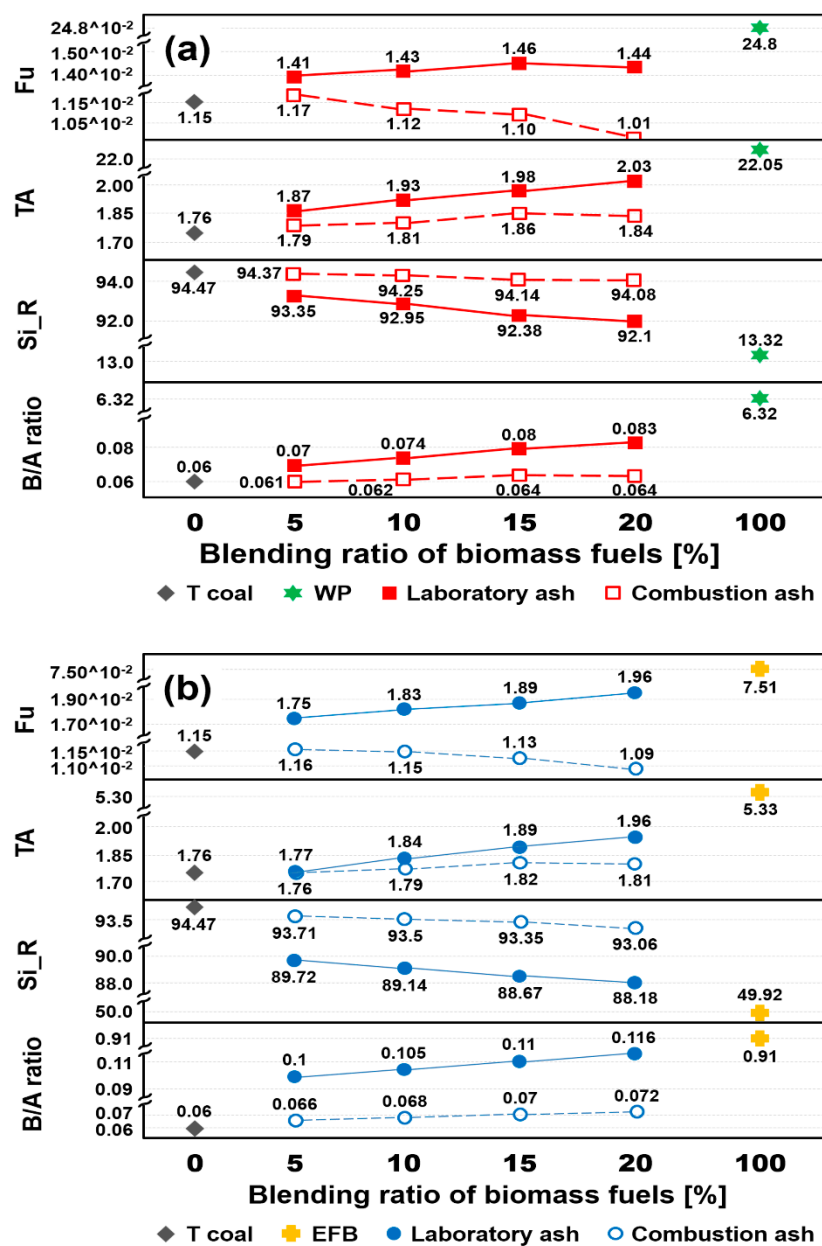

Figure 4. Trends of the traditional indices by X-ray fluorescence (XRF) results; (**a**) T coal + wood pellets (WP) and (**b**) T coal + empty fruit bunches (EFB) (B/A ratio, Si_R, TA, and Fu refer to base/acid ratio, silica percentage, total alkali, and fouling factor, respectively).

Table 2. Results of oxide analyses of laboratory and combustion ashes.

Components	Single Sample			T Coal + WP Blends				T Coal + EFB Blends			
	T Coal	WP	EFB	5%	10%	15%	20%	5%	10%	15%	20%
Laboratory ash											
SiO_2	66.27	8.75	39.30	65.72	65.43	65.13	64.92	63.39	63.11	62.79	62.44
Al_2O_3	26.69	3.54	9.22	26.31	26.25	26.07	25.94	26.09	25.81	25.62	25.43
TiO_2	1.24	0.25	0.45	1.21	1.19	1.18	1.22	1.26	1.25	1.29	1.31
Fe_2O_3	3.10	4.68	31.82	3.10	3.22	3.34	3.41	6.44	6.72	6.93	7.16
CaO	0.42	43.92	4.52	1.18	1.33	1.59	1.67	0.43	0.51	0.58	0.64
MgO	0.36	8.62	3.09	0.40	0.41	0.44	0.49	0.39	0.46	0.51	0.57
Na_2O	0.08	0	0	0.07	0.06	0.05	0.05	0.05	0.04	0.03	0.02
K_2O	1.68	22.05	5.33	1.80	1.87	1.93	1.98	1.72	1.80	1.86	1.94
P_2O_5	0.16	4.99	3.01	0.16	0.16	0.17	0.18	0.17	0.19	0.22	0.25
SO_3	0	3.20	3.26	0.05	0.08	0.10	0.14	0.06	0.11	0.17	0.24
Combustion ash											
SiO_2				66.16	66.10	66.01	65.96	65.88	65.71	65.57	65.39
Al_2O_3				26.69	26.64	26.60	26.62	26.51	26.43	26.41	26.33
TiO_2				1.22	1.23	1.23	1.22	1.23	1.24	1.22	1.22
Fe_2O_3				3.10	3.11	3.11	3.12	3.67	3.78	3.84	4.01
CaO		n.a. [a]		0.48	0.55	0.62	0.65	0.40	0.43	0.44	0.46
MgO				0.37	0.37	0.38	0.38	0.35	0.36	0.39	0.41
Na_2O				0.07	0.06	0.06	0.05	0.07	0.06	0.05	0.03
K_2O				1.72	1.75	1.80	1.79	1.69	1.73	1.77	1.78
P_2O_5				0.18	0.18	0.19	0.19	0.17	0.21	0.24	0.26
SO_3				0.01	0.01	0.01	0.02	0.03	0.05	0.07	0.11

[a] n.a.: Not analyzed.

Table 3. Summary of traditional ash deposition indices and associated criteria.

Indices	Formula	Criteria			
		Low	Medium	High	Severe
B/A ratio [32]	$(Fe_2O_3 + CaO + MgO + Na_2O + K_2O)/(SiO_2 + Al_2O_3 + TiO_2)$	<0.5	0.5–0.7	0.7–1.0	>1.0
Si_R [32]	$(SiO_2 \times 100)/(SiO_2 + Fe_2O_3 + CaO + MgO)$	>50	30–50	5.0–30	<5.0
TA [32]	$Na_2O + K_2O$	<2.0	2.0–3.0	3.0–4.0	>4.0
Fu [20]	$0.01 \times A_p$ [a] $\times$ B/A ratio $\times (Na_2O + 0.659 \times K_2O)$	<0.3	0.3–0.45	0.45–0.60	>0.6

[a] A_p: mass percentage of ash in fuel (or blends).

For the laboratory ash, the basic oxides are enriched as the blending ratio is increased, as shown in Table 2. This result is attributed to the unreacted mineral components remaining as-is (un-volatilized) at the low temperature. The effects of basic oxides from both biomass ashes are more evident using the traditional predictive indices and consequently affect the base/acid (B/A) ratio, total alkali (TA), and fouling factor (Fu) of the laboratory ash. As shown in Figure 4, the trends of indices derived from the XRF analysis using laboratory ash show that the slagging/fouling propensity continuously increases as the blending ratio of the biomass is increased.

Conversely, for the combustion ash obtained from the DTF experiments, acid oxides of the deposited ash samples are increased slightly compared to those of the laboratory ash. Particularly, the trends in B/A ratio and Fu identified in Figure 4 have very similar values within the criteria of Table 3, regardless of ash type. This is thought to correspond to the characteristics of the coal ash imparted by the minute fraction of biomass ash in the blending sample, although there is also an effect from the basic oxide of the biomass ash. The combustion ash is a good representation of a fly ash generated by a boiler. The combustion ash of the T coal blended with biomass mainly contains silica and alumina oxides (more than 90 wt%). Nevertheless, the chemical compositions of the laboratory ash and combustion ash vary only slightly with increasing biomass blending ratio, and neither ash type is significantly different from the T coal ash under the given blend conditions. This finding is in agreement with that of Kupka et al. [21], who observed that, excepting sulfur oxides, fly ash and crucible ash compositions, expressed as oxides, are generally consistent. Thus, Pronobis [12] proposed that the chemical composition of biomass during the co-combustion process is not clearly distinguishable from that of coal when the blending ratio for the thermal fraction of the biomass does not exceed 20%. In other words, the result implies that the chemical composition of biomass ash does

not influence that of the blend when the amount of biomass supplied is sufficiently small compared with that of the coal in terms of thermal input.

Tables 2 and 3 show that the deposition tendencies for both types of ashes meet the low-level criterion within each prediction index range. However, as the addition of biomass increases, the evaluations of the traditional prediction indices gradually increase, especially the TA index for the WP 20% blend. This implies that the blending ratio of coal and biomass whose basic oxides content reaches 90%, such as in the case of WP, should be carefully selected. The XRF results of this study show a difference between the chemical compositions of the ash types, which were generated at different temperatures according to the biomass co-combustion conditions, while the traditional prediction index results do not show a clear difference. Thus, a distinct deposition tendency cannot be confirmed. It is found, however, that as the biomass blending ratio increases, the deposition tendency is slightly increased regardless of ash type because the basic oxides are derived from the biomass ash.

As remarked by Kazagic and Smajevic [20], ash deposition evaluation based on laboratory ash analysis, including the calculation of traditional indices, shows poor reliability for biomasses, and laboratory results cannot be accepted as sufficiently reliable for evaluating the slagging and fouling propensities of biomasses. Therefore, this study performed further experiments using improved methods such as the TMA and DTF, as explained in the following sections.

3.2. Ash Melting Characteristics from TMA Experiments

To characterize the melting behavior of the laboratory ash, TMA experiments were performed for single-coal and blended samples. Figure 5 shows the shrinkage curves as a function of temperature for each raw sample.
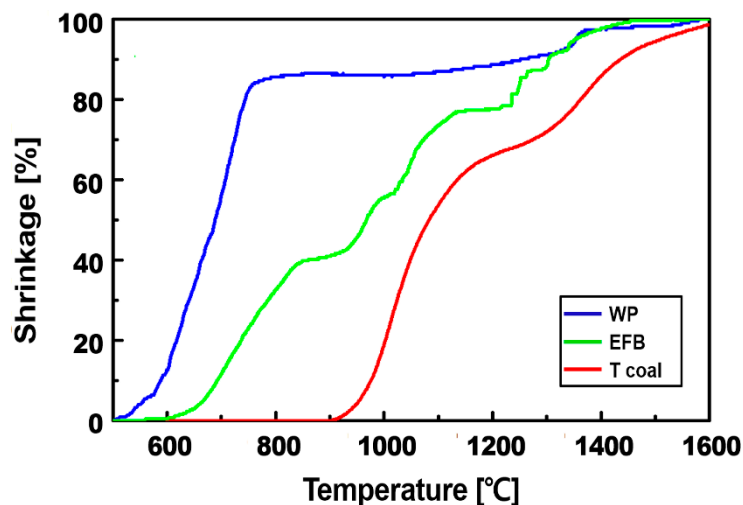

Figure 5. Shrinkage curves as a function of temperature for each raw sample.

The shrinkage curves shown in Figure 5 provide a good representation of the melting characteristics of each raw sample according to temperature. T coal is not completely melted at 1600 °C, which is the upper limit of the temperature in the TMA experiments performed. This is because T coal is a typical bituminous coal with acid oxide contents exceeding 90%, as seen from the XRF results [33].

Conversely, as demonstrated by the melting traces for both raw biomass samples, their melting reactions are completed at lower temperatures compared to that of T coal. For WP, the basic oxides content exceeds 85%, and T90% appears at a temperature lower than 1150 °C. For EFB, T90% appears at approximately 1300 °C, i.e., at a higher temperature than that of WP. This result is attributed to the ash components of WP, which have higher alkali contents than EFB, as shown in Table 2 and Figure 4.

When ash samples of blends are heated according to the thermal fraction, the melting trace of each blend follows that of raw T coal, which begins to melt at approximately 900 °C, as shown in Figure 6.

The melting temperatures for blended biomass are slightly lower or similar to that of raw T coal when the shrinkage is lower than T50% at all blending ratios. Conversely, when the shrinkage is higher than T50%, the melting temperatures are lower than that of raw T coal under all experimental conditions. It appears that the shrinkage is increased because the melting of raw biomasses is almost complete at temperatures lower than approximately 1200 °C, at which they are converted to the liquid phase. Moreover, this tendency is conspicuous in the results for EFB and when comparing the T75% value for the blend conditions; the decreased temperature for EFB blending is approximately 100 °C greater than that of the WP blends because EFB has higher ash contents despite its lower alkali content.
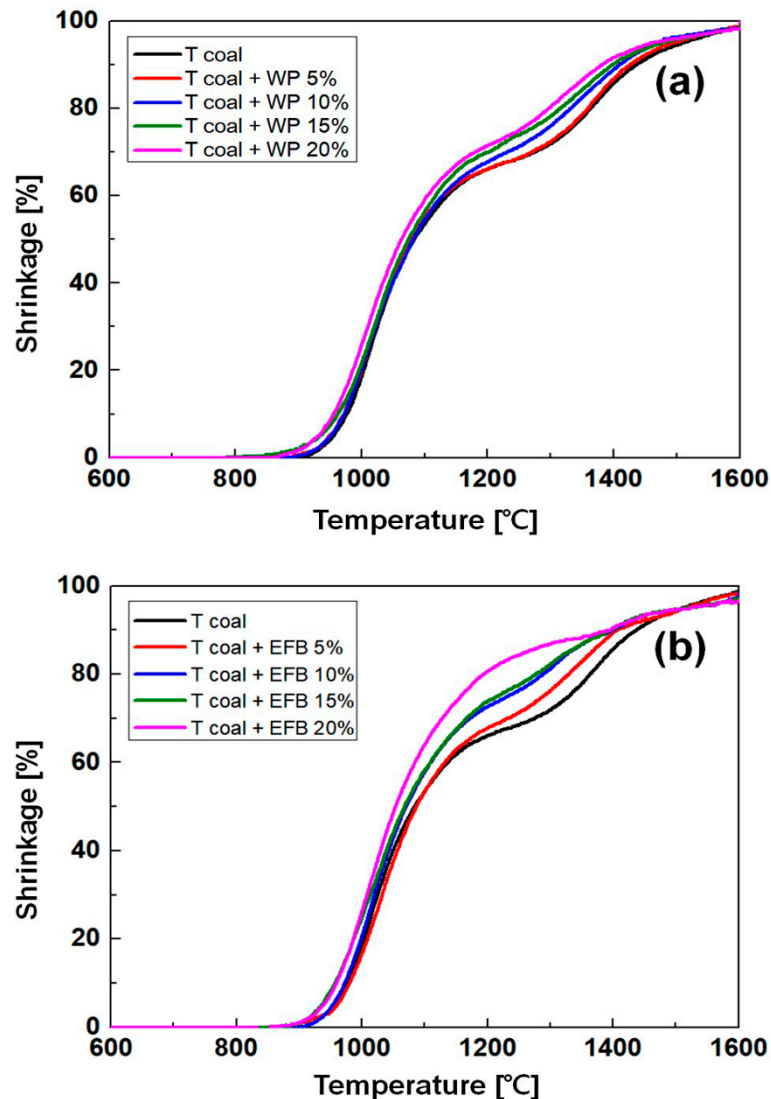

Figure 6. Shrinkage curves as a function of temperature for different blending ratios. (**a**) T coal + WP; (**b**) T coal + EFB.

Figure 7 illustrates the derivative trace of the results seen in Figure 6a,b. These graphs show the melting peak at which rapid melting occurs identified from the first derivative of the melting results derived from the shrinkage of biomass blending and the change in the peak temperature. The melting peaks of the biomass blends revealed in Figure 7a,b occur before approximately 1050 °C, which corresponds to a value between T25% and T50% of T coal.
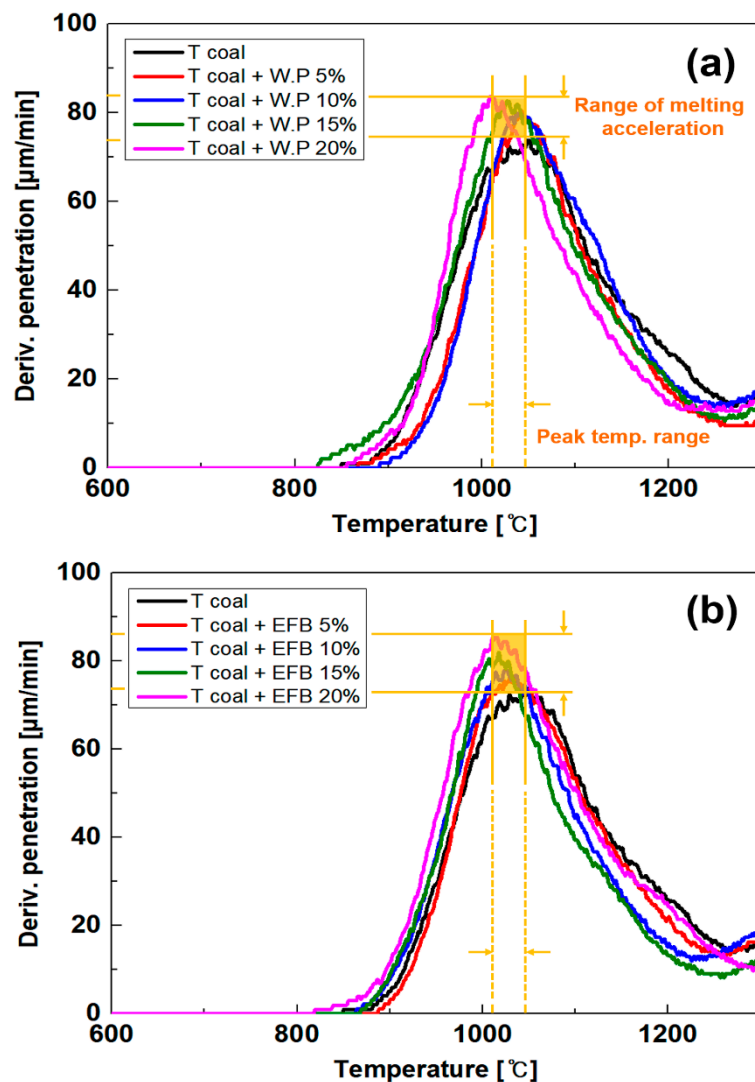
Figure 7. Derivative traces of the blend conditions derived from the TMA results; (**a**) T coal + WP; (**b**) T coal + EFB.

As shown in Figure 7, the melting peaks for the blends of both biomasses shift towards lower temperatures as the blending ratio increases based on the peak of T coal (at approximately 1050 °C). These peak temperatures are distributed between T25% and T50%, which is the shrinkage characteristic temperature of T coal. The melting is accelerated for the biomass as the peak height is gradually increased. Furthermore, in Figure 7a,b, the yellow peak distribution boxes indicate the melting intensity under a given blending ratio. The range of peak temperatures for both blends are not significantly different. However, the peak heights for EFB blends are higher than those of WP blends in a similar range of peak temperatures. Herein, the peak temperature is associated with the chemical composition of a sample and the height of the peak indicates a specific melting intensity. Since there is no difference in the chemical compositions of the ash of biomass blends and laboratory ash by XRF analysis, the melting intensity is affected by ash content according to blending conditions. As a result, the melting traces for biomass blending obtained with the TMA are confirmed. The melting temperature steadily decreases as the blending ratio of biomass increases, and this phenomenon is not reversed beyond a certain blending ratio. Therefore, this indicates that, as the biomass content in the blend increases, the melting temperature decreases and the slagging/fouling tendency can be expected to increase gradually.

3.3. Ash Deposition Characteristics from DTF Experiments

The DTF was used to examine the ash deposition of coal and biomass according to the experimental conditions. The deposited ash particles collected on the deposition probe during 1 h of experimentation and the deposition tendencies derived by the CE and GRE were used as the existing coal deposition indices. Figure 8 shows that co-combustion with WP and EFB generate relatively lower ash depositions than that of T coal alone. The single-coal deposition is evenly distributed over the entire area of the coupon and the deposited particles are stacked in a convex shape. In the case of biomass co-combustion, however, there is less deposition than in the case of single coal, and a narrow deposition distribution, with relatively low deposition on the side of the coupon, is observed along with a flatter deposit. Although these deposition images appear to show that the deposition is decreased compared to that of T coal as the blending ratio of the biomass is increased, it is difficult to confirm distinct trends.
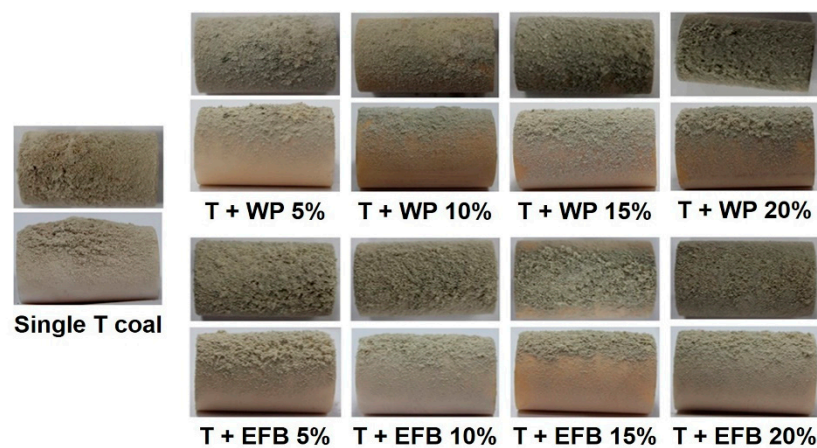

Figure 8. Images of ash collected on the deposit probe for different blend conditions and single combustion.

Figure 9 shows all the CE and GRE values obtained by co-combustion the biomass for all the blend conditions mentioned in Figure 3. The results show that, as the blending ratio of biomass (WP and EFB) increases, the deposition rate decreases for the 10% and 15% blends, but it begins to increase again with additional blending. In general, it is known that the ash in biomass contains significant amounts of alkali matter, which leads to a lower melting temperature, as shown in the TMA results. Most previous studies [34–36] reported that the addition of biomass increases ash deposition and attribute this result to the lower melting temperature and higher stickiness of biomass. Namkung et al. [37] also remarked that sticky particles tend to adhere to each other because of the partial melting characteristics of the particle surface and that increased biomass blending enhances ash deposition and agglomeration behavior. However, even though the blending ratio is increased, the deposition is initially decreased to a certain extent. This is why the ash contents of the biomasses (0.29% for WP and 2.77% for EFB) are much lower than that of T coal ash (17.11%). This finding is in agreement with those of previous studies. For example, Abreu et al. [15] reported that the co-combustion of coal with lower ash biomass does not pose operational problems related to the occurrence of slagging and fouling because the deposition rate decreases with increases in the biomass thermal input in the blend. In addition, similar effects have been reported by Kupka et al., who indicated that the ash deposition rate is influenced by ash input [21]. Therefore, these results point to the existence of additive and non-additive phenomena caused by lower ash contents and higher agglomeration effects during the co-combustion of coal with the biomasses.
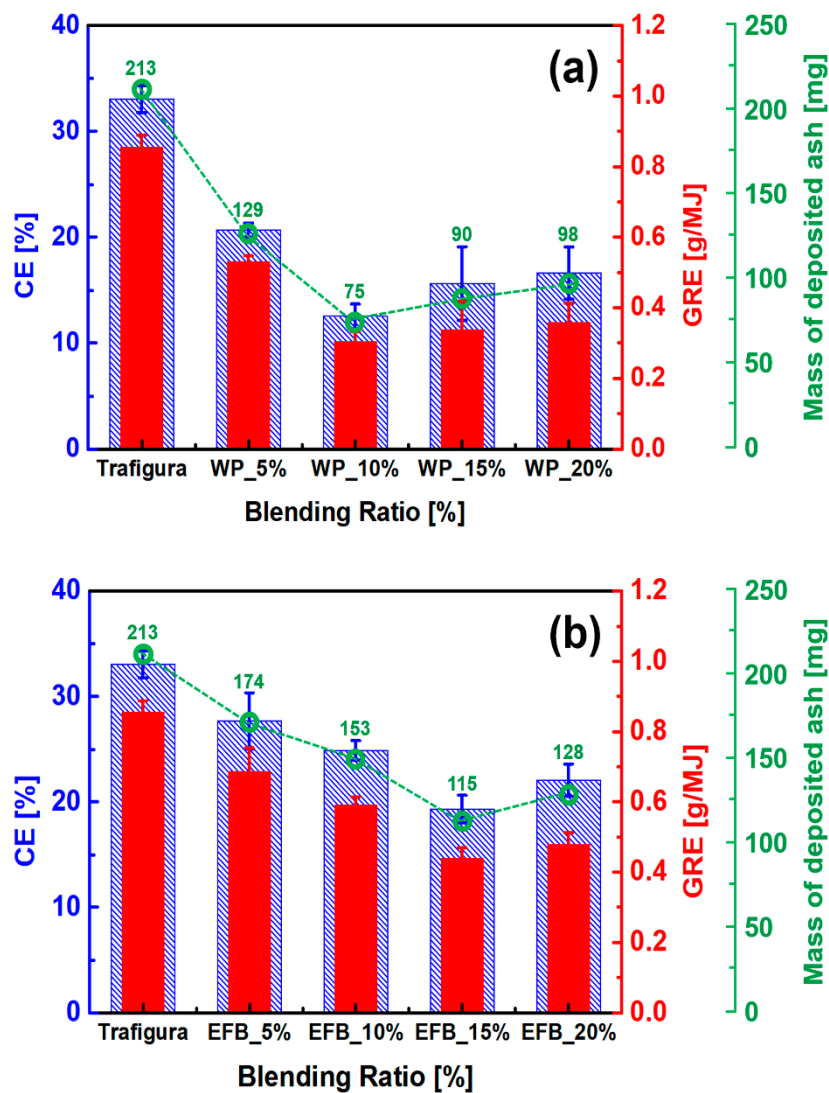
Figure 9. Values of capture efficiency (CE) and energy-based growth rate (GRE) for the blend conditions in the DTF; (**a**) T coal + WP; (**b**) T coal + EFB.

Figure 10 shows the normalized GRE values for the blend conditions in the DTF. Herein, GRE_{max} represents the ratio of the GRE values of other samples to the maximum GRE value. The GRE_{max} range of the WP blends is approximately 0.35–0.60, and that of the EFB blends is approximately 0.50–0.80. While the deposition of WP blends is less than half the deposition by the single combustion of T coal for all blending ratios except 5%, the deposition of EFB blends is higher than half the T coal deposition under all the co-combustion conditions. These results show that the deposition tendency with the co-combustion of EFB is higher than that of WP, unlike the predicted results using the chemical composition of the biomass revealed by XRF. In other words, the ash amounts of EFB, according to the feeding conditions, are approximately 10 times higher than those of WP, which demonstrates the influence of the deposition tendency. In addition, the reversal tendency of the EFB blend, i.e., the increase in deposition after the decrease, is changed at a higher blending ratio. This indicates that the deposition is more influenced by the feeding rate of the EFB than by its chemical composition when the amount of the biomass supplied is sufficiently small.
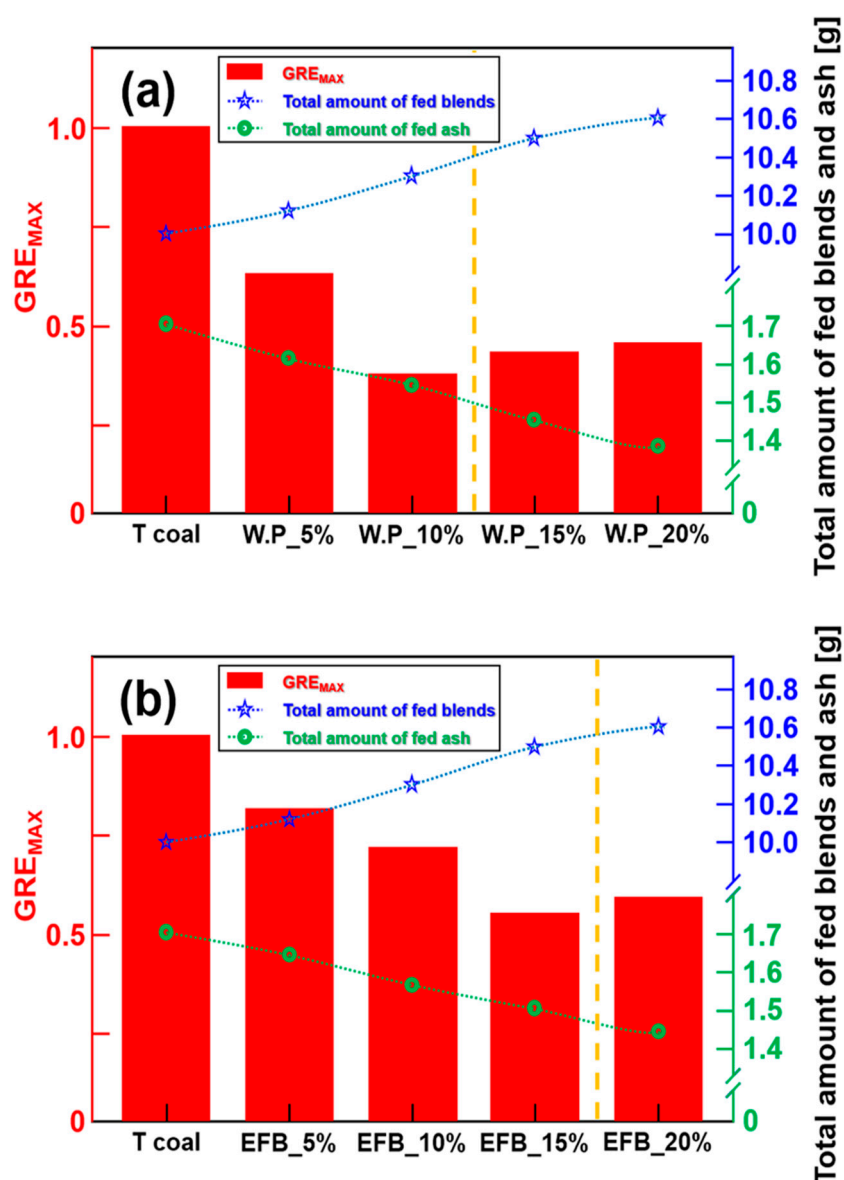
Figure 10. Normalized GRE values for blend conditions in the DTF; (**a**) T coal + WP; (**b**) T coal + EFB.

4. Conclusions

This study aimed to fundamentally investigate the ash deposition behavior during co-combustion of coal with two kinds of biomasses, WP and EFB, using TMA and DTF. The conclusions are as follows.

1. The laboratory and combustion ashes were analyzed using XRF and the slagging indices were derived using the chemical compositions. The ash compositions as per the results of XRF showed that the basic oxides were enriched as the blending ratio increased. Thus, the results of the XRF analysis showed that the deposition tendency continuously increases with an increasing biomass blending ratio, but the traditional indices for ash slagging propensity were insufficient for explaining the results because of their predictive limitations.

2. Ash melting characteristics were examined for the laboratory ash using a TMA. The % shrinkage traces of the raw fuel showed the individual melting characteristics of each fuel, and their % shrinkage traces for blends at T25% appeared to follow the melting characteristics of T coal. Conversely, the melting point clearly decreased after T50% as the blending ratio of the biomass increased. This indicates that the shrinkage accelerates when the melting of the biomass is almost complete and the biomass turns into a liquid phase. The TMA results revealed a decrease in

melting temperature with increasing WP and EFB blending, and the slagging/fouling tendency was expected to increase gradually.

3. The ash deposition characteristics revealed using the DTF showed a lower deposition tendency than that of single-coal combustion up to a blending ratio of 10% for WP and 15% for EFB. However, with further blending, a reversal was observed wherein the deposition tendency gradually increased. These results indicated the occurrence of additive and non-additive phenomena caused by the lower ash contents and higher agglomeration effects during the co-combustion of coal with the biomass.

4. These results indicate that an optimum blending ratio exists for the co-combustion of biomass with coal, and considering the ash contents as well as the agglomeration caused by the biomass ash indicated that a blending ratio of 10% for WP and 15% for EFB are the optimal conditions. The slagging tendency of EFB was worse than that of WP because of the ash contents of EFB.

5. WP have been researched extensively in Korea, but plant application of EFB can now be attempted. This study was performed in order to provide fundamental analysis and experiments using laboratory-scale apparatus, but further studies such as pilot and plant tests should be performed before applying EFB-derived fuels in power plants.

Author Contributions: Conceptualization, T.-Y.J. and C.-H.J.; data curation, T.-Y.J. and C.-H.J.; investigation, T.-Y.J., L.S., and J.-H.K.; methodology, T.-Y.J. and B.-H.L.; project administration, C.-H.J.; supervision, C.-H.J.; validation, T.-Y.J., L.S., J.-H.K., and B.-H.L.; visualization, T.-Y.J. and L.S.; writing—original draft, T.-Y.J.; writing—review and editing, T.-Y.J., B.-H.L., and C.-H.J.

Conflicts of Interest: The authors declare no conflict of interest.

References

1. Huang, C.W.; Li, Y.H.; Xiao, K.L.; Lasek, J. Cofiring characteristics of coal blended with torrefied Miscanthus biochar optimized with three Taguchi indexes. *Energy* **2019**, *172*, 566–579. [CrossRef]
2. Fuller, A.; Omidiji, Y.; Viefhaus, T.; Maier, J.; Scheffknecht, G. The impact of an additive on fly ash formation/transformation from wood dust combustion in a lab-scale pulverized fuel reactor. *Renew. Energy* **2019**, *136*, 732–745. [CrossRef]
3. Jeong, Y.-S. Assessment of alternative scenarios for CO_2 reduction potential in the residential building sector. *Sustainability* **2017**, *9*, 394. [CrossRef]
4. Park, H.-G.; Kim, C.-H. Do shifts in renewable energy operation policy affect efficiency: Korea's shift from FIT to RPS and its results. *Sustainability* **2018**, *10*, 1723. [CrossRef]
5. Lasek, J.A.; Kazalski, K. Sulfur self-retention during co-combustion of fossil fuels with biomass. *Energy Fuels* **2014**, *28*, 2780–2785. [CrossRef]
6. Liu, H.; Gibbs, B.M.; Hampartsoumian. The significance of rank on coal reburning for the reduction of NO in drop tube furnace. In Proceedings of the 8th International Symposium on Transport Phenomena in Combustion, San Francisco, CA, USA, 16–20 July 1995; pp. 329–340.
7. Lazaroiu, G.; Frentiu, T.; Mihaescu, L.; Mihaltan, A.; Ponta, M.; Frentiu, M.; Cordos, E. The synergistic effect in coal/biomass blend briquettes combustion on elements behavior in bottom ash using ICP-OES. *J. Optoelectron. Adv. M.* **2009**, *11*, 713–721.
8. Ali, U.; Akram, M.; Font-Palma, C.; Ingham, D.B.; Pourkashanian, M. Part-load performance of direct-firing and co-firing of coal and biomass in a power generation system integrated with a CO_2 capture and compression system. *Fuel* **2017**, *210*, 873–884. [CrossRef]
9. Shao, Y.; Wang, J.; Preto, F.; Zhu, J.; Xu, C. Ash deposition in biomass combustion or co-firing for power/heat generation. *Energies* **2012**, *5*, 5171–5189. [CrossRef]
10. Baxter, L.L. Ash deposition during biomass and coal combustion: A mechanistic approach. *Biomass Bioenerg.* **1993**, *4*, 85–102. [CrossRef]

11. Pronobis, M. The influence of biomass co-combustion on boiler fouling and efficiency. *Fuel* **2006**, *85*, 474–480. [CrossRef]

12. Pronobis, M. Evaluation of the influence of biomass co-combustion on boiler furnace slagging by means of fusibility correlations. *Bioresour. Bioenerg.* **2005**, *28*, 375–383. [CrossRef]

13. Theis, M.; Skrifvars, B.J.; Hupa, M.; Tran, H. Fouling tendency of ash resulting from burning mixtures of biofuels. Part 1: Deposition rates. *Fuel* **2006**, *85*, 1125–1130. [CrossRef]

14. Savolainen, K. Co-firing of biomass in coal-fired utility boilers. *Appl. Energy* **2003**, *74*, 369–381. [CrossRef]

15. Abreu, P.; Casaca, C.; Costa, M. Ash deposition during the co-firing of bituminous coal with pine sawdust and olive stones in a laboratory furnace. *Fuel* **2010**, *89*, 4040–4048. [CrossRef]

16. Sahu, S.G.; Chakraborty, N.; Sarkar, P. Coal-biomass co-combustion: An overview. *Renew. Sustain. Energy Rev.* **2014**, *39*, 575–586. [CrossRef]

17. Chen, X.; Tang, J.; Tian, X.; Wang, L. Influence of biomass addition on Jincheng coal ash fusion temperatures. *Fuel* **2015**, *160*, 614–620. [CrossRef]

18. Rushdi, A.; Sharma, A.; Gupta, R. An experimental study of the effect of coal blending on ash deposition. *Fuel* **2004**, *83*, 495–506. [CrossRef]

19. Febrero, L.; Granada, E.; Regueiro, A.; Miguez, J.L. Influence of combustion parameters on fouling composition after wood pellet burning in a lab-scale low-power boiler. *Energies* **2015**, *8*, 9794–9816. [CrossRef]

20. Kazagic, A.; Smajevic, I. Experimental investigation of ash behavior and emissions during combustion of Bosnian coal and biomass. *Energy* **2007**, *32*, 2009–2016. [CrossRef]

21. Kupka, T.; Mancini, M.; Irmer, M.; Webber, R. Investigation of ash deposit formation during co-firing of coal with sewage sludge, saw-dust and refuse derived fuel. *Fuel* **2008**, *87*, 2824–2837. [CrossRef]

22. Pimenidou, P.; Dupont, V. Characterisation of palm empty fruit bunch (PEFB) and pinewood bio-oils and kinetics of their thermal degradation. *Bioresour. Technol.* **2012**, *109*, 198–205. [CrossRef] [PubMed]

23. Madhiyanon, T.; Sathitruangsak, P.; Sungworagarn, S.; Pipatmanomai, S.; Tia, S. A pilot-scale investigation of ash and deposition formation during oil-palm empty-fruit-bunch (EFB) combustion. *Fuel Process. Technol.* **2012**, *96*, 250–264.

24. Guo, F.; Zhong, Z. Co-combustion of anthracite coal and wood pellets: Thermodynamic analysis, combustion efficiency, pollutant emissions and ash slagging. *Environ. Pollut.* **2018**, *239*, 21–29. [CrossRef]

25. Zeng, T.; Pollex, A.; Weller, N.; Lenz, V.; Nelles, M. Blended biomass pellets as fuel for small scale combustion appliances: Effect of blending on slag formation in the bottom ash and pre-evaluation options. *Fuel* **2018**, *212*, 108–116. [CrossRef]

26. Kim, G.-M.; Lee, D.-G.; Jeon, C.-H. Fundamental characteristics and kinetic analysis of lignocellulosic woody and herbaceous biomass fuels. *Energies* **2019**, *12*, 1008. [CrossRef]

27. Liu, Y.; Gupta, R.; Elliot, L.; Wall, T.; Fujimori, T. Thermomechanical analysis of laboratory ash, combustion ash and deposits from coal combustion. *Fuel Process. Technol.* **2007**, *88*, 1099–1107. [CrossRef]

28. Gupta, S.K.; Wall, T.F.; Creelman, R.A.; Gupta, R.P. Ash fusion temperatures and the transformations of coal ash particles to slag. *Fuel Process. Technol.* **1998**, *56*, 33–43. [CrossRef]

29. Lee, B.-H.; Kim, S.-G.; Song, J.-H.; Chang, Y.-J.; Jeon, C.-H. Influence of coal blending methods on unburned carbon and NO emissions in drop-tube furnace. *Energy Fuels* **2011**, *25*, 5055–5062. [CrossRef]

30. Barroso, J.; Ballester, J.; Ferrer, L.M.; Jimenez, S. Study of coal ash deposition in an entrained flow reactor: Influence of coal type, blend composition and operating conditions. *Fuel Process. Technol.* **2006**, *87*, 737–752. [CrossRef]

31. Blanchard, R. Measurements and modeling of coal ash deposition in an entrained flow reactor. Master's Thesis, Brigham Young University, Provo, UT, USA, 2008.

32. Lee, Y.-J.; Choi, J.-W.; Park, J.-H.; Namkung, H.; Song, G.-S.; Park, S.-J.; Lee, D.-W.; Kim, J.-G.; Jeon, C.-H.; Choi, Y.-C. Techno-economical method for the removal of alkali metals from agricultural residue and herbaceous biomass and its effect on slagging and fouling behavior. *ACS Sustain. Chem. Eng.* **2018**, *6*, 13056–13065. [CrossRef]

33. Wall, T.F.; Gupta, S.K.; Gupta, R.P.; Sanders, R.H.; Creelman, R.A.; Bryant, G.W. False deformation temperatures for ash fusibility associated with the conditions for ash preparation. *Fuel* **1999**, *78*, 1057–1063. [CrossRef]

34. Tortosa Masia, A.A.; Buhre, B.J.P.; Gupta, R.P.; Wall, T.F. Use of TMA to predict deposition behavior of biomass fuels. *Fuel* **2007**, *86*, 2446–2456. [CrossRef]

35. Priyanto, D.E.; Ueno, S.; Sato, N.; Kasai, H.; Tanoue, T.; Fukushima, H. Ash transformation by co-firing of coal with high ratios of woody biomass and effect on slagging propensity. *Fuel* **2016**, *174*, 172–179. [CrossRef]

36. Rong, H.; Wang, T.; Zhou, M.; Wang, H.; Hou, H.; Xue, Y. Combustion characteristics and slagging during co-combustion of rice husk and sewage sludge blends. *Energies* **2017**, *10*, 438. [CrossRef]

37. Namkung, H.; Lee, Y.-J.; Park, J.-H.; Song, G.-S.; Choi, J.-W.; Choi, Y.-C.; Park, S.-J.; Kim, J.-G. Blending effect of sewage sludge and woody biomass into coal on combustion and ash agglomeration behavior. *Fuel* **2018**, *225*, 266–276. [CrossRef]